ECCOMAS MSF 2019

4th International Conference on Multi-scale Computational Methods for Solids and Fluids

PROCEEDINGS

September 18-20, 2019
Sarajevo, Bosnia and Herzegovina

Editors:
A. Ibrahimbegovic, S. Dolarević, E. Džaferović,
M. Hrasnica, I. Bjelonja, M. Zlatar, K. Hanjalić

Organized by:

Faculty of Civil Engineering, University of Sarajevo,

Faculty of Mechanical Engineering, University of Sarajevo,
University of Technology of Compiègne, Alliance Sorbonne University, Paris

Supported by:

Academy of Sciences and Arts of Bosnia and Herzegovina, ANU BIH

Editors:

Adnan Ibrahimbegovic, Samir Dolarević, Ejub Džaferović,
Mustafa Hrasnica, Izet Bjelonja, Muhamed Zlatar, Kemal Hanjalić

Publisher: Faculty of Civil Engineering, University of Sarajevo,
Patriotske lige 30, 71000 Sarajevo, Bosnia and Herzegovina

Printed by: Štamparija Fojnica d.o.o.

Number of printed copies: 160

Date: September, 2019

ISBN: 978-9958-638-57-2

CIP - Katalogizacija u publikaciji
Nacionalna i univerzitetska biblioteka
Bosne i Hercegovine, Sarajevo

624:004(063)(082)

INTERNATIONAL Conference on Multi-scale Computational Methods for Solids and Fluids (4 ; 2019 ; Sarajevo)

Proceedings / 4th International Conference on Multi-scale Computational Methods for Solids and Fluids, Sarajevo, September 18-20, 2019 ; editors Adnan Ibrahimbegovic ... [et al.]. - Sarajevo : Faculty of Civil Engineering = Građevinski fakultet, 2019. - 417 str. : ilustr. ; 30 cm

Bibliografija uz svaki rad. - Registar.

ISBN 978-9958-638-57-2

COBISS.BH-ID 27453702

ELECTRO-MECHANICAL MODEL AND FINITE ELEMENT IMPLEMENTATION FOR DISCRETE LATTICE MODEL

Pablo Moreno-Navarro[1], Adnan Ibrahimbegovic[2], José L. Pérez-Aparicio[3]

[1] Laboratoire Roberval, Université de Technologie de Compiègne, pablo.moreno-navarro@utc.fr
[2] Laboratoire Roberval, Université de Technologie de Compiègne, adnan.ibrahimbegovic@utc.fr
[3] Mecánica Medios Continuos, Universitat Politècnica de València, jopeap@mes.upv.es

This work seeks to provide a formulation to simulate the microscopic behavior of a piezoelectric device and the corresponding macroscopic implementation into a finite element code for elastic and plastic regimes, such as [1]. To pull off this objective, a thermodynamically fully-consistent development of coupled mechanic and electric fields for ferroelectric materials has been established [2]. The formulation is implemented in the research Finite Element code FEAP [3].

The numerical modeling of the mechanical part of the structure is carried on using Voronoi cells [4]. The different cells are held together by cohesive links that are represented through 3D Timoshenko beams in finite element code, making computations faster than other structural representations. The degrees of freedom for the mechanic field are three displacements and three rotations:

$$\boldsymbol{u} = (u, v, w, \varphi, \psi, \theta)^{\mathsf{T}} \tag{1}$$

The strain vector associated with the corresponding degrees of freedom are:

$$\boldsymbol{\varepsilon} = (\varepsilon, \gamma_{x_2}, \gamma_{x_3}, \kappa_{x_1}, \kappa_{x_2}, \kappa_{x_3})^{\mathsf{T}} \tag{2}$$

And finally, the internal force vector:

$$\boldsymbol{F} = (N, V, W, M_{x_1}, M_{x_2}, M_{x_3})^{\mathsf{T}} \tag{3}$$

Regarding the electric field, the degree of freedom is the electric potential ϕ. For the beam model, only the axial component x_1 is relevant; thus, the definitions for the electric field E_{x_1} and the electric displacement D_{x_1} are scalars. Assuming the homogeneity of any variable within every section, we can define the electric charge as $Q_{x_1} = D_{x_1} A$, with A as the transverse area of the beam.

The constitutive equations for piezoelectric materials can be derived from the free-energy potential as in [8], from which we can retrieve:

$$\begin{aligned} \boldsymbol{\sigma} &= \mathcal{C}\boldsymbol{\varepsilon} - \boldsymbol{e}^{e}\boldsymbol{E} \\ \boldsymbol{D} &= \boldsymbol{\epsilon}\boldsymbol{E} + \boldsymbol{e}^{e}\boldsymbol{\varepsilon} \end{aligned} \tag{4}$$

The coefficients used in (4) are the stiffness tensor $\mathcal{C}$, the piezoelectric tensor $\boldsymbol{e}^{e}$, and the permittivity tensor $\boldsymbol{\epsilon}$, all of them obtained from material properties.

To reduce the previous model for beams, we need to account for the simplification done above: i) only a few components of primal variables are relevant, so are the corresponding material tensor entries; ii) the addition of rotational degrees of freedom for the mechanic field introduces new structural variables into the stiffness tensor and iii) only axial strain affects the axial electric variables and vice-versa.

The anisotropy introduced by the polarization is also treated. Polarization $\boldsymbol{P}$ is a macroscopic magnitude that accumulates the microscopic electric dipole moments in a material. Ferroelectric materials have permanent dipoles, generated due to a particular microstructure which generate remanent polarization $\boldsymbol{P}^{\mathsf{r}}$, with the only possibility of a change of orientation or domain switching [6].

A strong electric field has to be applied in the desired direction to switch the remanent polarization into any of the equilibrium positions. Also, a switch happens if compressive stress is applied in the direction of the current remanent polarization or traction in any of the corresponding transversal directions. The angle between the old and the new $\boldsymbol{P}^{\mathrm{r}}$ vector determines the two types of switching: 180° and 90°. An oriented electric field can cause both switches, whereas stress can only generate a 90° switch.

The selected criteria to determine whether a switch occurs is inspired by [7] where the combination of both electric field and stress is taken into account. It is an energy criterion at a microscopic level, and several possibilities have to be evaluated at the same time for both kinds of switch. A switch can take place if the following conditions meet:

$$\begin{aligned} \frac{\boldsymbol{E}\cdot\Delta\boldsymbol{P}^{\mathrm{r}}}{2\boldsymbol{E}\cdot\boldsymbol{P}^{\mathrm{s}}} &\geq 1\,, \quad \text{for } 180^\circ \text{ switch} \\ \frac{\boldsymbol{E}\cdot\Delta\boldsymbol{P}^{\mathrm{r}}}{\boldsymbol{E}\cdot\varepsilon^{\mathrm{s}}}+\frac{\boldsymbol{\sigma}\cdot\Delta\varepsilon^{\mathrm{r}}}{\boldsymbol{\sigma}\cdot\varepsilon^{\mathrm{s}}} &\geq 1\,, \quad \text{for } 90^\circ \text{ switch} \end{aligned} \tag{5}$$

where the increments $\Delta\boldsymbol{P}^{\mathrm{r}}$ and $\Delta\varepsilon^{\mathrm{r}}$ are the tensors of change for remanent polarization and strain respectively, and $\boldsymbol{P}^{s}$ and ε^{s} are the spontaneous values of remanent polarization or strain induced by internal microstructure. The above conditions need to be evaluated for each of the five alternative directions of polarization.

The manifestation of these remanent polarization, as well as the hypotheses assumed above, modify the continuum constitutive model into:

$$\begin{pmatrix} N \\ V \\ W \\ M_{x_1} \\ M_{x_2} \\ M_{x_3} \\ Q_{x_1} \end{pmatrix} = \begin{bmatrix} \breve{E}A & 0 & 0 & 0 & 0 & 0 & -e_{x_1,x_1}A \\ 0 & GA & 0 & 0 & 0 & 0 & 0 \\ 0 & 0 & GA & 0 & 0 & 0 & 0 \\ 0 & 0 & 0 & GJ & 0 & 0 & 0 \\ 0 & 0 & 0 & 0 & \breve{E}I & 0 & 0 \\ 0 & 0 & 0 & 0 & 0 & \breve{E}I & 0 \\ e_{x_1,x_1}A & 0 & 0 & 0 & 0 & 0 & \varepsilon_{x_1}A \end{bmatrix} \begin{pmatrix} \left(\varepsilon_{x_1}-\varepsilon^{\mathrm{r}}_{x_1}\right) \\ \gamma_{x_1,x_2} \\ \gamma_{x_1,x_3} \\ \kappa_{x_1} \\ \kappa_{x_2} \\ \kappa_{x_3} \\ E_{x_1} \end{pmatrix} + \begin{pmatrix} 0 \\ 0 \\ 0 \\ 0 \\ 0 \\ 0 \\ P^{\mathrm{r}}_{x_1}A \end{pmatrix} \tag{6}$$

where $\breve{E} = E\,(1-\nu)\,/\,[(1+\nu)\,(1-2\nu)]$ is the first term of the continuum stiffness tensor (with E as the Young's modulus and ν as the Poisson's coefficient), G is the shear modulus, J is the polar moment of inertia, I is the moment of inertia, ε_{x_1} is the permittivity in axial direction, and e_{x_1,x_1} is the piezoelectric coefficient. Notice that inertia moments are the same for x_2 and x_3 directions since the transversal area is assumed to be a circle.

These constitutive coefficients are also subjected to change with every polarization switch as in the previous solid model, which implies a change in $\breve{E}$, G, e_{x_1,x_1}, and ε_{x_1} [5]. The factor that modifies these properties from its non-polarized to its polarized value is the polarization multiplier m through the following linear distributions:

$$\begin{aligned} \breve{E} &= \breve{E}^{\mathrm{np}} + |m|\left(\breve{E}^{\mathrm{p}} - \breve{E}^{\mathrm{np}}\right) \\ G &= G^{\mathrm{np}} + |m|\left(G^{\mathrm{p}} - G^{\mathrm{np}}\right) \\ e_{x_1,x_1} &= e^{\mathrm{np}}_{x_1,x_1} + m\left(e^{\mathrm{p}}_{x_1,x_1} - e^{\mathrm{np}}_{x_1,x_1}\right) \\ \varepsilon_{x_1} &= \varepsilon^{\mathrm{np}}_{x_1} + |m|\left(\varepsilon^{\mathrm{p}}_{x_1} - \varepsilon^{\mathrm{np}}_{x_1}\right) \end{aligned} \tag{7}$$

where the superscripts np and p stand for non-polarized and polarized values of each coefficient and $|m|$ is the absolute value of m. The values for remanent polarization and remanent strain are also a function of this multiplier as follows:

$$\begin{aligned} P^{\mathrm{r}}_{x_1} &= m\,P^{\mathrm{s}}_{x_1} \\ \varepsilon^{\mathrm{r}}_{x_1} &= |m|\,\varepsilon^{\mathrm{s}}_{x_1} \end{aligned} \tag{8}$$

A numerical difficulty arises when the switch in polarization is implemented as a Heaviside step once one of the conditions in (5) is met. This abrupt change can lead to oscillating residual norms in the finite element method due to the uncertainty of the beams getting simultaneously polarized.

A smooth correction to this Heaviside step is proposed for these two models through the hyperbolic tangent function. The idea is to make a bijective function between electric field and electric displacement, removing any possible uncertainty and introducing a smooth change of slope. Once the polarization switches, the constitutive model changes to represent hysteresis behavior.

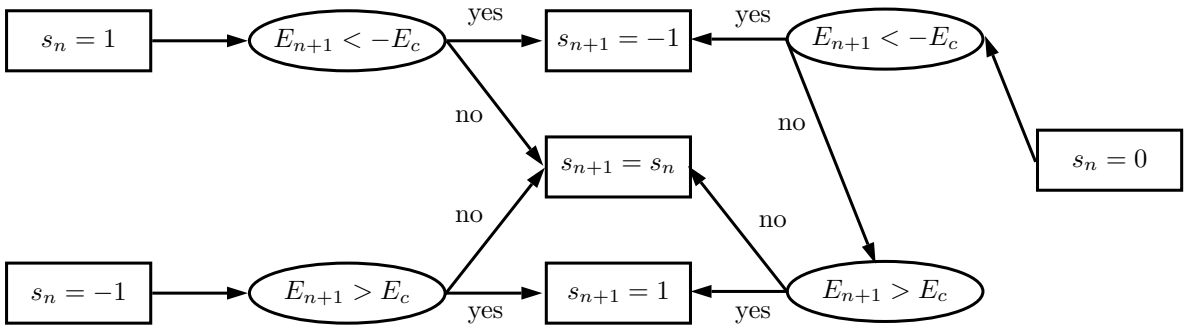

Figure 1: Diagram of decision to select the switch-state for the next time step s_{n+1} based on its previous value s_n and the current value of electric field E_{n+1}

This decision diagram is represented in Figure 1, where every beam starts with the zero switch-state $s_n = 0$. It will remain in this state until the beam reaches the coercive electric field E_c or $-E_c$. This forces the switch-state to change in the next time step to either $s_{n+1} = 1$ or $s_{n+1} = -1$, denoting positive or negative polarization respectively. After the beam is polarized, the beam can only switch to the opposite polarized state (180°) once it reaches the opposite value of the coercive electric field, i.e., $-E_c$ for $s_n = 1$ and E_c for $s_n = -1$.

The three states of polarization are implemented in this model, although it can be noticed that once a beam is polarized either positive or negative, it cannot return to the zero-state. This first model is rather simple but allows us to get a good approximation in macroscopic electric displacement $\boldsymbol{D}$.

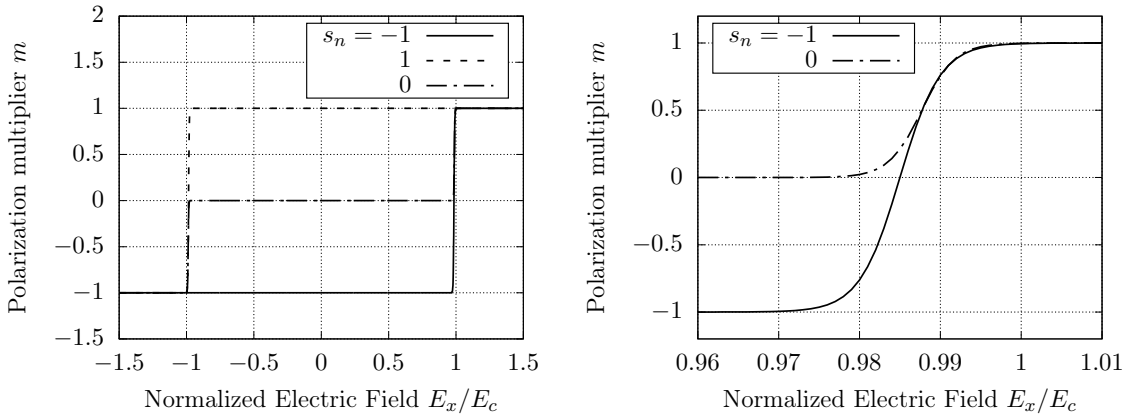

Figure 2: Left, smoothed polarization multiplier m curves for all three previous state of polarization s_n with the chosen $a = 200$. Right, detail of curves $|s_n| = 1$ and $a = 244$ for $s_n = 0$.

Although the switch-state changes suddenly, the polarization multiplier is a smooth function, continuum and derivable, by means of the hyperbolic tangent. This multiplier, drawn in Figure 2, depends on the current axial electric field in the beam E_{n+1} and the switch from the previous time step s_n as follows:

$$m_{n+1}(E_{n+1}, s_n) = \frac{1-s_n}{2} \tanh\left[\frac{a(s_n)}{E_c}(E_{n+1} - E_c) + 3\right] + \frac{1+s_n}{2} \tanh\left[\frac{a(s_n)}{E_c}(E_{n+1} + E_c) - 3\right] \quad (9)$$

The geometry of the numerical example is a cube, with sides of 20 cm. The top and bottom faces have prescriptions of the voltage of $V = 0$ and $V = V_t(t)$, respectively. The voltage at the top is triangular,

starting with a value of 0 to $V_{\max} = 0.2$ MV, then $-V_{\max}$ and returning to $V_{\max}$. In planes $x_1 = 0$, $x_2 = 0$, and $x_3 = 0$, the corresponding perpendicular displacement is prescribed to simulate symmetry boundary conditions. Rotation degrees of freedom are left free. All switches are set initially to zero. The material properties are extracted from [9].

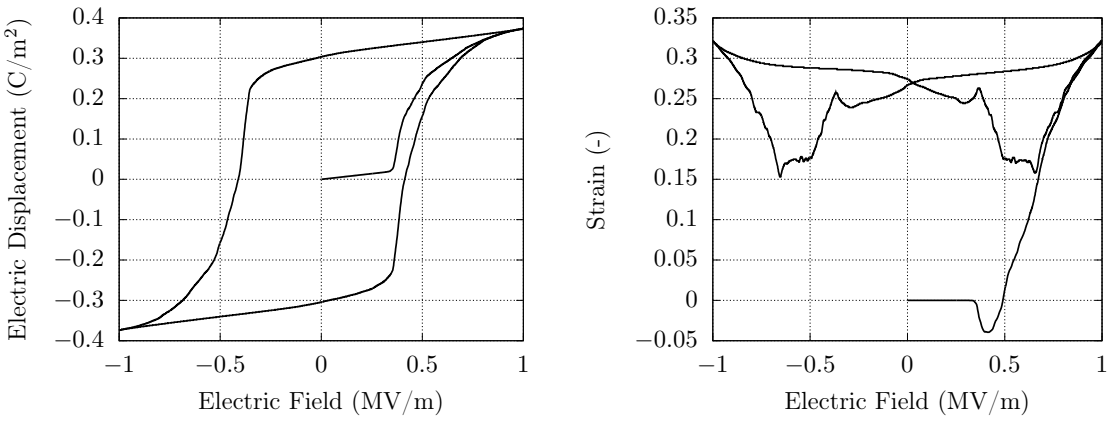

Figure 3: Averaged vertical electric displacement and strain obtained for the numerical example

The electric and mechanic variables calculated with the beam model have to be expressed in the global frame and averaged with the volume to interpret the macro response of the material using:

$$\bar{\xi} = \frac{\int_{\Omega^e} \xi \mathrm{d}\Omega}{\int_{\Omega^e} \mathrm{d}\Omega} \tag{10}$$

In Figure 3, the averaged response for the numerical example is plotted, where the typical hysteresis loops for electric displacement and strain can be appreciated. One of the limitations of this method is that cannot capture transversal effects with accuracy, but the axial variables are close to the continuum model.

References

[1] JL Pérez-Aparicio, R Palma, and P Moreno-Navarro. Elasto-thermoelectric non-linear, fully coupled, and dynamic finite element analysis of pulsed thermoelectrics. *Applied Thermal Engineering*, 107:398–409, 2016.

[2] A Ibrahimbegovic. *Nonlinear solid mechanics: theoretical formulations and finite element solution methods*, volume 160. Springer Science & Business Media, 2009.

[3] OC Zienkiewicz and RL Taylor. *The Finite Element Method, vols. I, II, III*. Elsevier, 2005.

[4] E Hadzalic, A Ibrahimbegovic and S Dolarevic. Theoretical formulation and seamless discrete approximation for localized failure of saturated poro-plastic structure interacting with reservoir. *Computers & Structures*, in press, 2019.

[5] M Labusch, M-A Keip, V Shvartsman, DC Lupascu and J Schröder. On the influence of ferroelectric polarization states on the magneto-electric coupling in two-phase composites. *Computers & Structures*, 36:73–87, 2016.

[6] CA Balanis. *Advanced engineering electromagnetics*. John Wiley & Sons, 1999.

[7] M-A Keip, P Steinmann, and J Schröder. Two-scale computational homogenization of electro-elasticity at finite strains. *Computer Methods in Applied Mechanics and Engineering*, 278:62–79, 2014.

[8] P Moreno-Navarro, A Ibrahimbegovic, and JL Pérez-Aparicio. Linear elastic mechanical system interacting with coupled thermo-electro-magnetic fields. *Coupled System Mechanics*, 7(1):5–25, 2018.

[9] SC Hwang, CS Lynch, and RM McMeeking. Ferroelectric/ferroelastic interactions and a polarization switching model. *Acta Metallurgica Materials*, 43(5):2073–2084, 1995.

Proceedings:
E. Hadžalić

Local organizing committee:
A. Ibrahimbegovic, S. Dolarević, E. Džaferović, M. Hrasnica, I. Bjelonja,
M. Zlatar, K. Hanjalić

E. Hadžalić, E. Hajdo, I. Imamović, E. Karavelić, J. Medić, S. Suljević,
R.A. Mejia-Nava, P. Moreno-Navarro, I. Rukavina, C.U. Nguyen, S. Dobrilla